Eur. Phys. J. B **4**, 447–457 (1998)

THE EUROPEAN PHYSICAL JOURNAL B

Strongly correlated Falicov–Kimball model in infinite dimensions

B.M. Letfulov[a]

Institute of Metal Physics, Ural division of Russian Academy of Sciences, Kovalevskaya str. 18, Ekaterinburg, 620219, Russia

Received: 15 October 1997 / Accepted: 11 March 1998

Abstract. In this paper we have examined the strongly correlated Falicov–Kimball model in infinite dimensions with the help of a diagrammatic technique for the Hubbard X-operators. This model is represented by the simplified $t-J$ model with introduced intra-atomic level energy ε^0 for localized particles. For the Bethe lattice with $z \to \infty$, we have found that the obtained equations for the band Green's function and self-energy coincide with the corresponding Brandt–Mielsch equations taken at $U \to \infty$, and are resolved in analytical form both in the homogeneous phase and in the chessboard phase. In the latter case we have obtained the equation for the order parameter defining the chessboard-like distribution of localized particles. Instability of the homogeneous phase and properties of the chessboard phase are investigated in detail. In particular, it is found that the temperature dependence of the chessboard order parameter has reentrant behaviour for some range of values of ε^0.

PACS. 71.10.Fd Lattice fermion models (Hubbard model, etc.) – 71.45.Lr Charge-density-wave systems

1 Introduction

The research of electron correlation effects induced by strong intra-atomic interactions remains at the center of attention of investigators after three decades. On the one hand, this interest is conditioned by discoveries of new materials such as the heavy-fermion compounds or the high-temperature superconductors. But from a theoretical point of view the long standing attention to the strongly correlated electron systems is due to the unsatisfactory state of their theory.

Indeed, in the theory of the mentioned systems there are many methods and approaches for calculation of different physical quantities. However, some of these methods such as the method of decoupling Green's functions or the slave-boson method contain uncontrolled approximations. Other methods (for example, diagrammatic technique for the Hubbard X-operators) are very cumbersome and hard. On the whole we have many contradictory calculations and a few steady and logically correct results.

In our opinion, the exact solution of the Falicov–Kimball model in infinite dimensions [1–3] is one of the most interesting results in the physics of the strongly correlated systems. Further development of the theory of this model in infinite dimensions was made in the following papers [4–8].

The spinless Falicov–Kimball model [9] was originally introduced to describe the metal-insulator transition in systems with localized (f-) and itinerant (d-) electrons. It has also attracted interest as a model for electron-induced formation of crystalline order [10], and for other applications. Its Hamiltonian has the form

$$\mathcal{H} = -\mu \sum_i d_i^\dagger d_i + (\varepsilon^0 - \mu) \sum_i f_i^\dagger f_i + U \sum_i d_i^\dagger d_i f_i^\dagger f_i + \sum_{\langle i,j \rangle} t_{ij} d_i^\dagger d_j. \qquad (1.1)$$

Here $d_i^\dagger$ ($f_i^\dagger$) is the creation operator of d- (f-) electrons, U is the intra-atomic interaction energy. The chemical potential μ constrains the total number of itinerant and localized electrons. The important parameter of the theory ε^0 sets the energy level of a localized electron with respect to the middle of the itinerant electron band. When $\varepsilon^0 = 0$, we have the simplified Hubbard model in which electrons with, for example, $\downarrow$-spin projection are localized.

In spite of its simplicity the Falicov–Kimball model reveals a series of non-trivial properties. In particular, the authors of the papers [10–12] have found that the Falicov–Kimball system can undergo a phase transition at some finite temperature T_c, and in the ground state there is a chessboard-like distribution of the localized electrons. The phase transition at $T = T_c$ can occur in a d-dimensional lattice with $d \geq 2$.

Brandt and Mielsch [1–3] have obtained the exact solution of the Falicov–Kimball model in infinite dimensions by mapping the lattice problem on an atomic problem with an additional time-dependent field acting on the itinerant electrons. They were able to calculate the transition temperature dependence on interaction U for different occupation numbers of localized electrons and to study the chessboard phase. One can show [4,5] that the Brandt-Mielsch equations for the itinerant electron Green's

[a] e-mail: Barri.Letfulov@imp.uran.ru

function and self-energy are the equations of the dynamical mean-field theory and the description of transition into the chessboard phase is the true mean-field description.

It should be noted that the Brandt-Mielsch solution has been used by several authors as the background for the approximate solution of the $d = \infty$ Hubbard model [13–15] and $d = \infty$ $t-J$ model [16]. The general idea of these approaches is to treat the electrons of some spin projection as moving in the field of the electrons of another spin projection, considered to be frozen and static. This is the idea of molecular field approximation.

In this paper we study the strongly correlated limit ($U \gg W$, W is the bandwidth of itinerant electrons) of the Falicov–Kimball model in infinite dimensions. One can show that the Hamiltonian of the strongly corelated Falicov–Kimball model is written as

$$\mathcal{H} = \mathcal{H}_0 + \mathcal{H}_{int}, \tag{1.2}$$

$$\mathcal{H}_0 = -\mu \sum_i X_i^{++} + (\varepsilon^0 - \mu) \sum_i X_i^{--}, \tag{1.3}$$

$$\mathcal{H}_{int} = \mathcal{H}_t + \mathcal{H}_J$$

$$= \sum_{\langle i,j \rangle} t_{ij} X_i^{+0} X_j^{0+} - \sum_{\langle i,j \rangle} J_{ij} X_i^{++} X_j^{--}. \tag{1.4}$$

Here, X_i^{pq} is the Hubbard X-operator describing the transition of the lattice site with number i from $|q\rangle$-state to the $|p\rangle$-state; $p, q = 0, +, -$. $|+\rangle$-state ($|-\rangle$-state) is associated with the state of the itinerant (localized) electrons. $|0\rangle$-state is the state without electrons. The quantities t_{ij} and J_{ij} are assumed to be nonzero for the nearest neighbours, and $J = t^2/U$.

In infinite dimensions the second term $\mathcal{H}_J$ in (1.4) is decoupled as

$$\mathcal{H}_J = -\sum_{\langle i,j \rangle} J_{ij} \Big(\langle X_i^{++} \rangle X_j^{--} + X_i^{++} \langle X_j^{--} \rangle \Big). \tag{1.5}$$

Therefore, it is convenient to add this term to $\mathcal{H}_0$, so that $\mathcal{H}_{int} = \mathcal{H}_t$ and

$$\mathcal{H}_0 = \sum_{i\sigma} \varepsilon_{i\sigma} X_i^{\sigma\sigma}, \tag{1.6}$$

where

$$\varepsilon_{i+} = -\mu - \sum_j J_{ij} \langle X_j^{--} \rangle,$$

$$\varepsilon_{i-} = \varepsilon^0 - \mu - \sum_j J_{ij} \langle X_j^{++} \rangle. \tag{1.7}$$

Using the rebuilt Hamiltonian, in Section 2 we define the set of equations for the band Green's function and self-energy by diagrammatic technique for the Hubbard X-operators. In this section we also give the expression for the $f-f$ correlation function from which one can obtain the equation for the transition temperature. The main results of this section coincide with the Brandt-Mielsch results [1,2] taken at $U \to \infty$. In Section 3 we show that the equations obtained in Section 2 can be resolved in analytical form for the Bethe lattice with $z \to \infty$, where z is the number of nearest neighbours. Using the $f-f$ correlation function for the Bethe lattice, we study in this section instability of the homogeneous phase. In Section 4 we consider the chessboard phase with the help of the equation for the chessboard phase order parameter. This equation can be obtained for the Bethe lattice in analytical form too. Some concluding remarks are given in the last section.

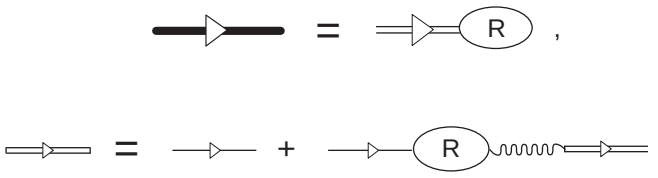

Fig. 1. General diagram of the structure of band Green's function.

2 Band Green's function and general equations

In order to obtain the equations for the band Green's function

$$\mathcal{G}(i, i'; \tau - \tau') = -\langle T \tilde{X}_i^{0+}(\tau) \tilde{X}_{i'}^{+0}(\tau') \rangle, \tag{2.1}$$

we shall use the diagrammatic technique for the Hubbard X-operators (on this subject see Refs. [17,18]).

Because of the complicated anticommutation relation

$$X_i^{0+} X_{i'}^{+0} + X_{i'}^{+0} X_i^{0+} = F_i^{+0} \delta_{ii'}, \quad F_i^{+0} = 1 - X_i^{--} \tag{2.2}$$

the general expression for the function (2.1) in our model has the form shown in Figure 1, where the transfer integral $t_{ii'}$ is associated with the wavy line and the "zero" Green's function

$$G^0(i, i'; i\omega_s) = \frac{\delta_{ii'}}{i\omega_s - \varepsilon_{i+}} \tag{2.3}$$

is associated with the thin solid line.

It is seen from Figure 1 that in contrast to the ordinary diagram technique for the standard Fermi operators the expression for function (2.1) contains so-called "end" part $R(i, i'; \tau - \tau')$, so that

$$\mathcal{G}(i, i'; i\omega_s) = \sum_{i_1} G(i, i_1; i\omega_s) R(i_1, i'; i\omega_s), \tag{2.4}$$

where $G(i, i'; i\omega_s)$, represented in Figure 1 by the double solid line, obeys the equation

$$G(i, i'; i\omega_s) = G^0(i, i'; i\omega_s)$$

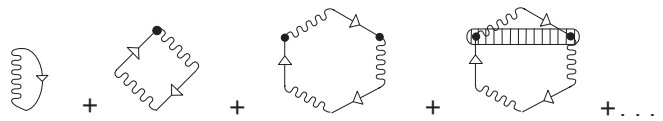

Fig. 2. Diagram series for $P_s(i,i)$.

$$+\sum_{i_1,i_2} G^0(i,i_1;i\omega_s)\Xi(i_1,i_2;i\omega_s)G(i_2,i';i\omega_s), \qquad (2.5)$$

where

$$\Xi(i,i';i\omega_s)=\sum_{i_1} R(i,i_1;i\omega_s)t_{i_1i'}. \qquad (2.6)$$

In accordance with the general ideology of the theory of itinerant electron systems in infinite-dimensional space [19,20], we shall consider that

$$R(i,i';i\omega_s)=R(i,i;i\omega_s)\delta_{ii'}. \qquad (2.7)$$

Therefore,

$$\mathcal{G}_s(i,i')=G_s(i,i')R_s(i',i'),$$

$$\Xi_s(i,i')=R_s(i,i)t_{ii'} \qquad (2.8)$$

where we have used the following designations

$$\mathcal{G}(i,i';i\omega_s)\equiv\mathcal{G}_s(i,i'),$$

$$G(i,i';i\omega_s)\equiv G_s(i,i') \qquad (2.9)$$

and so on.

One can show that the usual Dyson self-energy part $\Sigma_s(i,i)$ in equation

$$\mathcal{G}_s^{-1}(i,i')=\Big(i\omega_s-\varepsilon_{i+}\Big)\delta_{ii'}-t_{ii'}-\Sigma_s(i,i)\delta_{ii'} \qquad (2.10)$$

has the form

$$\Sigma_s(i,i)=\frac{R_s(i,i)-1}{G_s^0(i,i)R_s(i,i)}\cdot \qquad (2.11)$$

Therefore, in our approach the problem of calculation of $\Sigma_s(i,i)$ is replaced by one of $R_s(i,i)$.

Let us find the equation for "end" part $R_s(i,i)$. It is convenient for this purpose to introduce the new quantity

$$P(i,i';\tau-\tau')=\sum_{i_1} t_{ii_1}G(i_1,i';\tau-\tau'). \qquad (2.12)$$

Diagrams, taking into account for $P(i,i';\tau-\tau')$ in the case $i=i'$, are in Figure 2 where unshaded ovals with the n bold points inside correspond to "zero" cumulants:

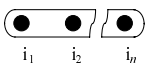

$$= D^0(i_1,i_2,\dots,i_n) \qquad (2.13)$$

$$=(-1)^{n-1}\frac{\partial^{n-1}}{\partial x_{i_1-}^{n-1}}\langle F_{i_1}^{+0}\rangle_0\delta_{i_1i_2}\delta_{i_2i_3}\dots\delta_{i_{n-1}i_n},$$

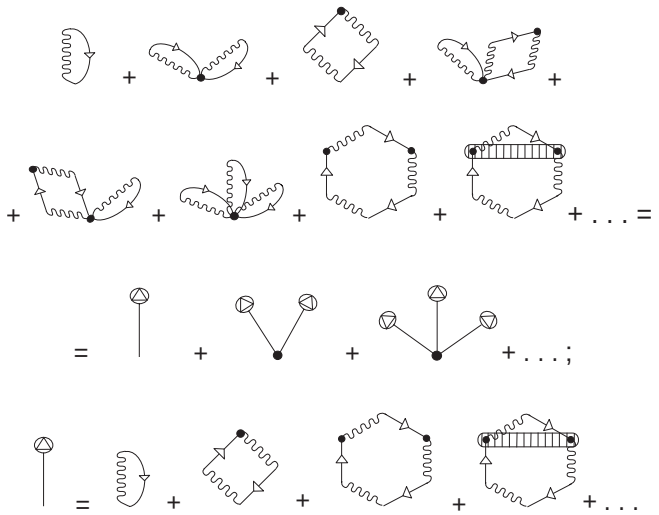

Fig. 3. Rebuilt diagram series for $P_s(i,i)$ and a diagram series for $\mathcal{P}_s(i,i)$.

$$\langle F_i^{+0}\rangle_0=1-\langle X_i^{--}\rangle_0\equiv 1-w_i^0, \qquad (2.14)$$

$$w_i^0=\frac{e^{x_{i-}}}{1+e^{x_{i+}}+e^{x_{i-}}},\quad x_{i\sigma}=-\beta\varepsilon_{i\sigma},\quad \beta=\frac{1}{T}\cdot \qquad (2.15)$$

The series in Figure 2 is a sum of diagrams with external vertices having equal site numbers and with every possible cumulant bonds replaced by those ones taken in the exact local approximation. These exact local cumulants $D(i_1,i_2,\dots,i_n)$ are presented in Figure 2 by shaded ovals.

The possibility of the exact calculation of the cumulants in local approximation is caused by the fact that

$$[\mathcal{H},F_i^{+0}]=0$$

and that the exact average of T-product of F_i^{+0}-operators taken in the Heisenberg presentation does not depend on Matsubara times.

Thus,

$$\equiv D(i)=1-w_i,$$

$$\equiv D(i_1,i_2)=w_{i_1}\big(1-w_{i_1}\big)\delta_{i_1i_2},$$

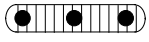

$$\equiv D(i_1,i_2,i_3)=-w_{i_1}\big(1-w_{i_1}\big)\big(1-2w_{i_1}\big)$$

$$\delta_{i_1i_2}\delta_{i_2i_3} \qquad (2.16)$$

and so on, where

$$w_i=\langle X_i^{--}\rangle. \qquad (2.17)$$

All these formulae are easily calculated with the help of equations (2.13–2.15) with the change of w_i^0 by w_i. The exact equation for w_i will be given later.

To sum the series in Figure 2 let us rebuild it, so that as a result we can obtain the series shown in Figure 3. For this, taking into account the circumstance that the summation is taken over lattice sites of internal vertices, we select in each diagram in Figure 2 the contributions with

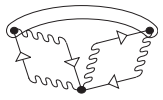

Fig. 4. Diagrams of this type are equal to zero in limit $d \to \infty$.

internal vertices coinciding by site number with external vertex in every possible way. It is necessary to use relations (2.16) when combining. Thus, in Figure 3 at first, third, seventh and eight diagrams of the series for $P_s(i,i)$ no one among the internal vertices can coincide with external vertex, and the quantity $\mathcal{P}(i,i;i\omega_s) \equiv \mathcal{P}_s(i,i)$, shown in the same figure, is the sum of the diagrams of just such a type.

After the mentioned rebuilding, graphs of the type shown in Figure 4 turn out to be omitted in Figure 3. But they are equal to zero in the limit $d \to \infty$ or $z \to \infty$, because diagrams of such a type have at least one pair of internal vertices that are connected by local cumulants. (Method of estimating of diagrams with respect to $1/d$ or $1/z$ is discussed, for example, in Ref. [21]).

The series for $P_s(i,i)$ in Figure 3 is summed easily in terms of functions $\mathcal{P}_s(i,i)$:

$$P_s(i,i) = \mathcal{P}_s(i,i)\frac{1 - w_i\mathcal{P}_s(i,i)}{1 - \mathcal{P}_s(i,i)}\,. \tag{2.18}$$

On the other hand, from the evident equations for $P_s(i,i')$ and $\mathcal{P}_s(i,i')$:

$$P_s(i,i') = P_s^0(i,i') + \sum_{i_1} P_s^0(i,i_1)R_s(i_1,i_1)P_s(i_1,i'), \tag{2.19}$$

$$\mathcal{P}_s(i,i') = P_s^0(i,i') + \sum_{i_1 \neq i'} P_s^0(i,i_1)R_s(i_1,i_1)\mathcal{P}_s(i_1,i'), \tag{2.20}$$

where

$$P_s^0(i,i') = \frac{t_{ii'}}{i\omega_s - \varepsilon_{i+}},$$

one can obtain

$$\mathcal{P}_s(i,i) = \frac{P_s(i,i)}{1 + R_s(i,i)P_s(i,i)}\,. \tag{2.21}$$

By substituting (2.21) into (2.18) we obtain the desired equation for $R_s(i,i)$:

$$R_s(i,i) = \frac{1 - w_i}{1 + P_s(i,i)\Big[R_s(i,i) - 1\Big]}\,. \tag{2.22}$$

After some manipulations with the help of the equation (2.22), one can obtain the following useful relations

$$\mathcal{G}_s(i,i) = G_s(i,i) - w_i G_s^0(i,i), \tag{2.23}$$

$$R_s(i,i) = \frac{\mathcal{G}_s(i,i)}{G_s(i,i)} \tag{2.24}$$

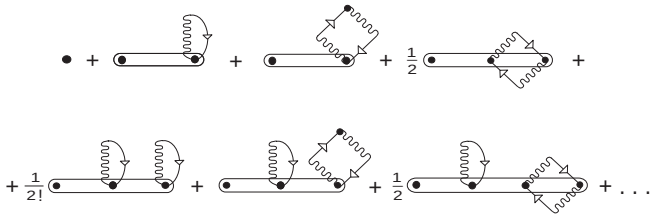

Fig. 5. Diagram series for w_i.

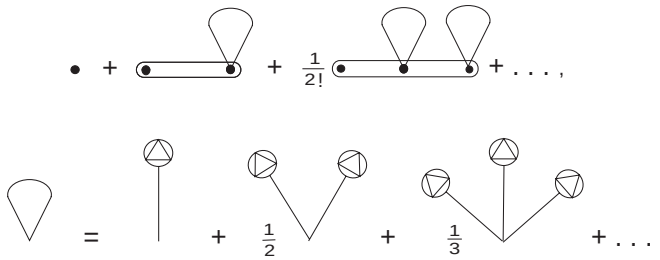

Fig. 6. Rebuilt diagram series for w_i.

and as a result we have

$$\Sigma_s(i,i) = -\frac{w_i}{\mathcal{G}_s(i,i)}\,. \tag{2.25}$$

This is the Brandt-Mielsch result for the self-energy part of the band Green's function for the case $U \to \infty$.

For the calculation of the probability of finding the site with number i occupied by localized electron (f-occupation number)

$$w_i = \langle X_i^{--}\rangle = \frac{\langle T\tilde{X}_i^{--}(\tau)\sigma(\beta)\rangle_0}{\langle\sigma(\beta)\rangle_0}, \tag{2.26}$$

where $\sigma(\beta)$ is the temperature scattering matrix, let us examine the series shown in Figure 5. After rebuilding this series, analogous in practice to the one done for function $P_s(i,i)$ it is possible to obtain the series shown in Figure 6. This series is a Taylor series and is summed easily. As a result we obtain

$$w_i = \frac{e^{x_{i-}+\lambda_i}}{1 + e^{x_{i+}} + e^{x_{i-}+\lambda_i}}, \tag{2.27}$$

where

$$\begin{aligned}\lambda_i &= -\sum_s \ln\Big(1 - \mathcal{P}_s(i,i)\Big) \\ &= -\sum_s \ln\Big(Z_s(i,i)G_s^0(i,i)\Big),\end{aligned} \tag{2.28}$$

$$Z_s(i,i) = \frac{1}{\mathcal{G}_s(i,i)} + \Sigma_s(i,i). \tag{2.29}$$

Now let us calculate the $f-f$ correlation function (with the factor $1/T$)

$$\begin{aligned}\chi^{--}(i,i) &= \frac{1}{T}\langle(X_i^{--} - w_i)(X_{i'}^{--} - w_{i'})\rangle \\ &= -\frac{dw_i}{d\varepsilon_{i'}^0}, \qquad \varepsilon_{i'}^0 \to \varepsilon^0\end{aligned} \tag{2.30}$$

for the case of the homogeneous phase, where $w_i = w$. For this aim, we shall use the method of Brandt and Mielsch [1].

From equations (2.30, 2.27) one can obtain directly

$$\frac{dw_i}{d\varepsilon^0_{i'}} = -\frac{1}{T}w(1-w)\delta_{ii'} + w(1-w) \times \sum_{i_1} J_{ii_1} \sum_s \frac{d\mathcal{G}_s(i_1,i_1)}{d\varepsilon^0_{i'}} - w(1-w)\sum_s \frac{1}{Z_s}\frac{dZ_s(i,i)}{d\varepsilon^0_{i'}}. \tag{2.31}$$

Taking into account that

$$\frac{dZ_s(i,i)}{d\varepsilon^0_{i'}} = \sum_{i_1} \frac{dZ_s(i,i)}{dw_{i_1}}\frac{dw_{i_1}}{d\varepsilon^0_{i'}} \tag{2.32}$$

and

$$\frac{d\mathcal{G}_s(i,i)}{d\varepsilon^0_{i'}} = \sum_{i_1} \frac{d\mathcal{G}_s(i,i)}{dw_{i_1}}\frac{dw_{i_1}}{d\varepsilon^0_{i'}} \tag{2.33}$$

we have

$$\frac{dw_i}{d\varepsilon^0_{i'}} = -\frac{1}{T}w(1-w)\delta_{ii'} - w(1-w) \times \sum_s \sum_{i_1}\left(\frac{1}{Z_s}\frac{dZ_s(i,i)}{dw_{i_1}} - \sum_{i_2} J_{ii_2}\frac{d\mathcal{G}_s(i_2,i_2)}{dw_{i_1}}\right)\frac{dw_{i_1}}{d\varepsilon^0_{i'}}. \tag{2.34}$$

From (2.29) we find by implicit differentiation

$$\frac{dZ_s(i,i)}{dw_{i'}} = \frac{\partial\Sigma_s}{\partial w}\delta_{ii'} + \left(-\frac{1}{\mathcal{G}_s^2} + \frac{\partial\Sigma_s}{\partial\mathcal{G}_s}\right)\frac{d\mathcal{G}_s(i,i)}{dw_{i'}}\,. \tag{2.35}$$

Substituting (2.35) into (2.34), we can see that it is necessary to calculate the total derivative $d\mathcal{G}_s(i,i)/dw_{i'}$ yet. With the help of the relation

$$\mathcal{G}_s(i,i) = \sum_{i_1,i_2} \mathcal{G}_s(i,i_1)\mathcal{G}_s^{-1}(i_1,i_2)\mathcal{G}_s(i_2,i)$$

and (2.10) one can obtain for it the following equation

$$\frac{d\mathcal{G}_s(i,i)}{dw_{i'}} = \sum_{i_1}\mathcal{G}_s(i,i_1)\mathcal{G}_s(i_1,i) \times \left(\frac{\partial\Sigma_s}{\partial w}\delta_{i_1i'} - J_{i_1i'} + \frac{\partial\Sigma_s}{\partial\mathcal{G}_s}\frac{d\mathcal{G}_s(i_1,i_1)}{dw_{i'}}\right). \tag{2.36}$$

After the Fourier transformation we have the final expression for $\chi^{--}(\mathbf{q})$ as

$$\chi^{--}(\mathbf{q}) = \frac{w(1-w)}{D(\mathbf{q})}, \tag{2.37}$$

where

$$D(\mathbf{q}) = T + wn_+J(\mathbf{q}) + wT\sum_s \frac{1+\mathcal{G}_sJ(\mathbf{q})}{w\chi^0_s(\mathbf{q}) - \mathcal{G}_s^2} \times \Big\{\mathcal{G}_s^2 - \chi^0_s(\mathbf{q}) - (1-w)\mathcal{G}_sJ(\mathbf{q})\chi^0_s(\mathbf{q})\Big\}, \tag{2.38}$$

$$\chi^0_s(\mathbf{q}) = \frac{1}{N}\sum_{\mathbf{k}}\mathcal{G}_s(\mathbf{k})\mathcal{G}_s(\mathbf{k}+\mathbf{q}), \tag{2.39}$$

$\mathcal{G}_s(\mathbf{k})$ and $J(\mathbf{q})$ are the Fourier transforms of $\mathcal{G}_s(i,i')$ and $J_{ii'}$, $n_+ = \langle X_i^{++}\rangle$ is the itinerant electron concentration.

3 Bethe lattice. Instability of the homogeneous phase

In contrast to the case of Gaussian density of states utilized by Brandt and Mielsch [1,2], the equations

$$\mathcal{G}_s = \int_{-\infty}^{\infty} \frac{\rho_0(\varepsilon)d\varepsilon}{i\omega_s + \mu + J^*w - \varepsilon - \Sigma_s} \tag{3.1}$$

and

$$\Sigma_s = -\frac{w}{\mathcal{G}_s}, \tag{3.2}$$

where $J^* = Jz = const$, can be resolved for the case of the Bethe lattice with $z\to\infty$ in analytical form.

Indeed, in this case

$$\rho_0(\varepsilon) = \frac{4}{\pi W}\sqrt{1-\left(\frac{2\varepsilon}{W}\right)^2}, \quad -\frac{1}{2}W < \varepsilon < \frac{1}{2}W, \tag{3.3}$$

W is the bandwidth, the integral in (3.1) is taken, and with the help of (3.2) one can obtain the following expressions for $\mathcal{G}_s$:

$$\mathcal{G}_s = \frac{8}{W}\left\{i\omega_s + \mu - \sqrt{(i\omega_s+\mu)^2 - \frac{1}{4}W^2(1-w)}\right\} \tag{3.4}$$

and for Σ_s:

$$\Sigma_s = -\frac{1}{2}\left(\frac{w}{1-w}\right) \times \left\{i\omega_s + \mu + \sqrt{(i\omega_s+\mu)^2 - \frac{1}{4}W^2(1-w)}\right\}, \tag{3.5}$$

$$\mathrm{Im}\Sigma(\omega+i\delta) = \begin{cases} -\frac{1}{2}\left(\frac{w}{1-w}\right)\sqrt{a^2-(\omega+\mu)^2}, & -a < \omega+\mu < a \\ 0, & -a \geq \omega+\mu \geq a \end{cases} \tag{3.6}$$

where

$$a = \frac{1}{2}W\sqrt{1-w} \tag{3.7}$$

is the halfwidth of the correlated band.

The chemical potential in (3.4) was renormalized by $\mu + J^*w \to \mu$. The equation for it has the form

$$n = w + n_+ = w + T\sum_s \mathcal{G}_s$$

or

$$n = w + (1-w)\frac{2}{\pi}\int\limits_{-1}^{1} dx\sqrt{1-x^2}f(ax), \tag{3.8}$$

where n is the total electron concentration and

$$f(z) = \frac{1}{\exp[\beta(z-\mu)]+1}$$

is the Fermi–Dirac function.

In the case of the Bethe lattice the quantity w (f-occupation number) obeys the following equation

$$w = \frac{1}{\exp[\beta(\varepsilon^f-\mu)]+1}, \tag{3.9}$$

where

$$\varepsilon^f = \varepsilon^0 - J^*(n-2w) + \frac{1}{\pi}\int\limits_0^{\pi} dt \ln\left(1+e^{\beta(\mu-a\cos t)}\right) \tag{3.10}$$

is the renormalized f-particle intra-atomic level. The expression (3.8) is obtained from (2.27) after the calculation of λ_i with the help of (2.28, 3.4, 3.5).

At $T = 0$ the equations (3.8, 3.10) are represented by

$$n = \frac{1}{2}(1+w) + (1-w)\frac{1}{\pi}\left\{\frac{\mu}{a}\sqrt{1-(\mu/a)^2} + \arcsin\frac{\mu}{a}\right\} \tag{3.11}$$

and

$$\varepsilon^f = \varepsilon^0 - J^*(n-2w) + \frac{1}{2}\mu + \frac{1}{\pi}\left\{\mu\arcsin\frac{\mu}{a} + \sqrt{a^2-\mu^2}\right\}, \tag{3.12}$$

where $\mu \le a$.

Now let us discuss the obtained results. Firstly, $n \le 1$ at any temperature and any chemical potential. When $w = 1$, $n = 1$. Secondly, the f-occupation number w in the case $T = 0$ can attain only three values: $w = 1$ when

$$\varepsilon^0 < -J^*, \tag{3.13}$$

$w = 1/2$ when

$$\varepsilon^f = \mu \tag{3.14}$$

and $w = 0$ under the following condition

$$\varepsilon^0 - J^*n + \frac{1}{\pi}\left(\mu\arcsin\frac{2\mu}{W} + \sqrt{W^2/4-\mu^2}\right) - \frac{1}{2}\mu > 0. \tag{3.15}$$

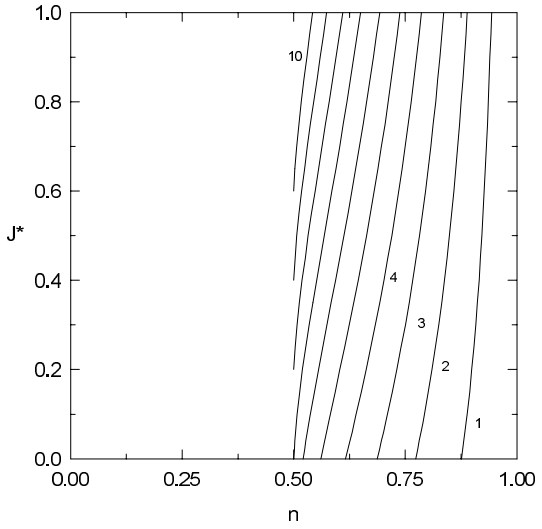

Fig. 7. Curves on which $w = 0.5$ for different values of ε^0. $1 - \varepsilon^0 = 0.1$; $2 - \varepsilon^0 = 0.2$ and so on to $10 - \varepsilon^0 = 1.0$.

(A discussion of the importance of the behaviour of w for interpretation of valence transitions can be found in Refs. [22,23]).

The case (3.14) of the pinning of the chemical potential μ at the localized particle level was considered in [7] for the Lorentzian density of band states. Let us note in connection with it that the imaginary part of itinerant electrons self-energy in [7] contains the multiplier $w(1-w)$ which is not equal to zero only in the case of (3.14). As a result, the Fermi-liquid behaviour in this case is invalidated [7].

For the case of the Bethe lattice and $U \gg W$, the self-energy of itinerant electrons contains the multiplier $w/(1-w)$ (see Eq. (3.5)). When $w = 0$, the subsystem of itinerant electrons presents itself as a free electron gas. When $w = 1$, the concentration of itinerant electrons is equal to zero and $\mathcal{G}_s = 0$. At $T = 0$ the self-energy is a non-trivial quantity only when $w = 1/2$.

It should be noted that the multipliers $w(1-w)$ and $w/(1-w)$ are characteristic ones for the Falicov–Kimball model. As we shall see in future, the multiplier $w(1-w)$ defines the behaviour of the transition temperature to a chessboard phase. Therefore, let us examine the conditions (3.13–3.15) in detail.

For our case the curves, on which equation (3.14) is satisfied, are shown in Figure 7 for different ε^0 (all the energetical quantities in figures are given in units of $W/2$). It is seen that the f-occupation number w can attain the value $w = 1/2$ in the cases of non-positive ε^0 only. In the $\varepsilon^0 = 0$ case $w = 1/2$ on the $n = 1$ line. This is a symmetric case. As an explanation of the Figure 7, let us note that in the $w = 1/2$ case $n \ge 1/2$ for any ε^0.

For negative ε^0 the f-occupation number can attain the value $w = 1$ too. This fact is easily seen from condition (3.13). In this case the value of n is always equal to 1.

Figure 8 shows the set of curves defining the boundaries of regions in which $w = 0$ for different values of ε^0 (see the condition (3.15)). On the left, from the corresponding curves, $w = 0$ for given ε^0. On the right, from

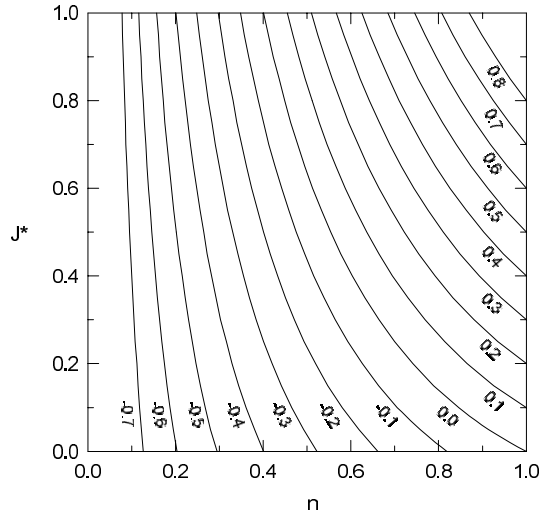

Fig. 8. Curves on the left from which $w = 0$ for different values of ε^0. A number near a curves shows the values of ε^0.

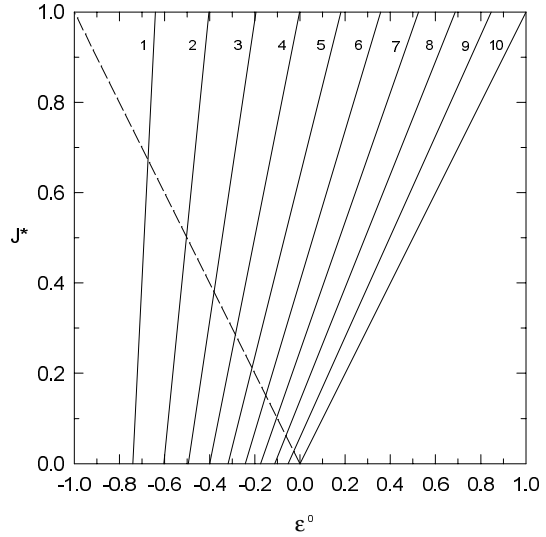

Fig. 9. Curves on the right from which $w = 0$ for different values of n. 1 – $n = 0.1$; 2 – $n = 0.2$ and so on to 10 – $n = 1.0$. On the left from the dashed line $w = 1$.

the one with the exceptions of the range $J^* < -\varepsilon^0$ on the $n = 1$ axis, where $w = 1$, and the corresponding curve, where $w = 1/2$ (see Fig. 7), the equation (3.9) at $T = 0$ has no solution. The crossing of a $J^* = const$ line with the $w = 0$ curve for given ε^0 defines a critical value of the total electron concentration n_c depending on J^* and ε^0, such that at $n < n_c$ the value of w is equal to zero and the one at $n > n_c$ is undefined in the sense of the existence of a solution for the equation (3.9) at $T = 0$.

Figure 9 shows the same condition (3.15) for different n on the phase plane which is defined by the other quantities: J^* and ε^0. The crossing of a $J^* = const$ line with the $w = 0$ curve for given n defines a critical value ε_c^0 depending on J^* and n, such that the value of w is equal to zero at $\varepsilon^0 > \varepsilon_c^0$. The dashed line in the same figure shows the right boundary of region, where $w = 1$.

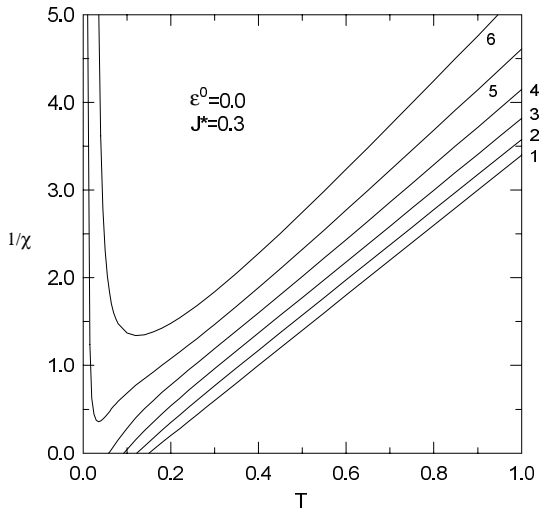

Fig. 10. Temperature dependence of the inverse $f-f$ susceptibility. 1 – $n = 1.0$; 2 – $n = 0.9$; 3 – $n = 0.8$; 4 – $n = 0.7$; 5 – $n = 0.6$; 6 – $n = 0.5$.

At the discussion of the condition (3.15), we have noted that in the phase space (J^*, ε^0, n) there is the region in which the equation (3.9) at $T = 0$ has no solution w. This fact can mean that in this region the homogeneous phase is unstable with respect to another phase with another equation for w.

Let us consider in connection with this the $f-f$ correlation function (2.37) with $\mathbf{q} = \mathbf{Q} \equiv (\pi, \pi, \dots)$. In this case we have

$$\chi_s^0(\mathbf{Q}) = \frac{\mathcal{G}_s}{i\omega_s - \varepsilon_+ - \Sigma_s} \tag{3.16}$$

and

$$D(\mathbf{Q}) = T - 2w(1-w)f(0)J^* - w(1-w)$$

$$\times \left[\left(\frac{1}{4}W\right)^2 - (1-w)\left(J^*\right)^2\right] \frac{2}{a\pi} \int_{-1}^{1} \frac{dz}{z} \sqrt{1-z^2} f(az). \tag{3.17}$$

Temperature dependence of the inverse susceptibility in the homogeneous phase is shown in Figure 10 for $\varepsilon^0 = 0$, $J^* = 0.3$ and different values of n. Intersection of the curves of inverse susceptibility with the axis of abscissa gives the transition temperature T_c to chessboard phase. It is seen that at the small values of n susceptibility has a cusp and for such values of n the homogeneous phase is stable.

For $n = 1$ (the symmetric case) the $f-f$ susceptibility has the Curie–Weiss-like behaviour. When n is decreased, the transition temperature T_c is decreased too. Let us note that with decrease of n, the critical behaviour of susceptibility is changed. Curie–Weiss-like behaviour with the critical exponent $\gamma = 1$ is replaced by the critical behaviour with $\gamma < 1$. An analogous situation takes place in the theory of the $s-f$ model (Kondo lattice) with the

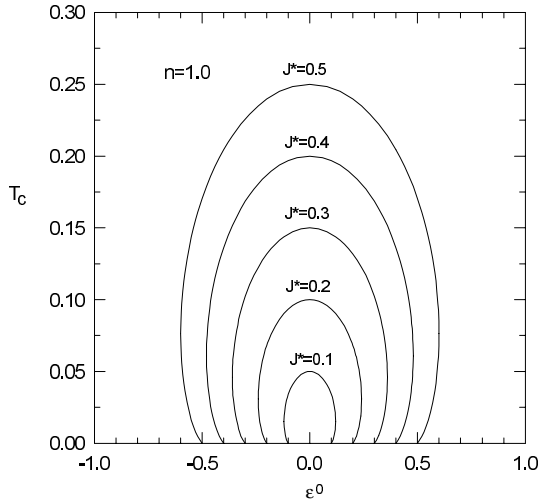

Fig. 11. ε^0 dependence of the transition temperature T_c for different values of J^*.

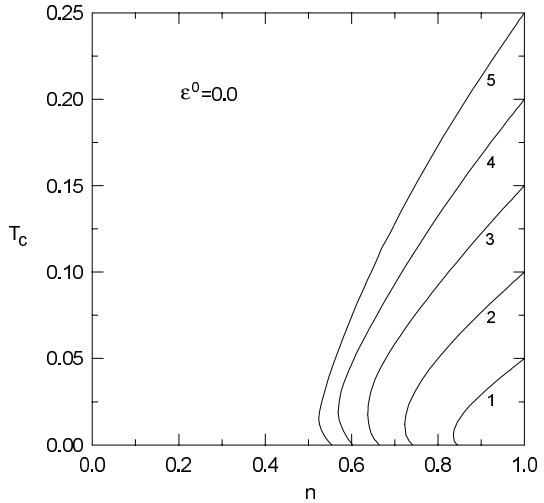

Fig. 12. n dependence of the transition temperature T_c for different values of J^*. 1 – $J^* = 0.1$; 2 – $J^* = 0.2$; 3 – $J^* = 0.3$; 4 – $J^* = 0.4$; 5 – $J^* = 0.5$.

infinitely large $s-f$ interaction (double exchange mechanism of indirect exchange between localized spins [24,25]).

Figure 11 shows dependence of the critical temperature T_c on energy ε^0 for $n = 1$ and different values of J^*. The curves in Figure 11 are symmetric with respect to $\varepsilon^0 = 0$. For a given J^* the critical temperature attains a maximum value at $\varepsilon^0 = 0$. In this symmetric case

$$T_c = \frac{1}{2}J^*. \tag{3.18}$$

Two symmetric values of ε^0 for given J^*, at which $T_c = 0$, coincide with the critical values of ε_c^0 defined from Figure 9 for the corresponding value of J^*.

Let us note that the ε^0 dependence of T_c has in addition two symmetric values ε_*^0 and $-\varepsilon_*^0$, such that in the ranges

$$\varepsilon_c^0 < \varepsilon^0 < \varepsilon_*^0 \quad \text{and} \quad -\varepsilon_*^0 < \varepsilon^0 < -\varepsilon_c^0. \tag{3.19}$$

The equation $D(\mathbf{Q}) = 0$ has two solutions for T_c: T_{c1} and T_{c2}. At $\varepsilon^0 = |\varepsilon_*^0|$ we have $T_{c1} = T_{c2} = T_c^*$. This situation will be discussed in the next section.

In closing this section we want to give the n dependence of T_c for $\varepsilon^0 = 0$ and different values of J^*. This dependence is shown in Figure 12. The value of n for given J^*, at which $T_c = 0$, coincides with the critical value n_c defined from Figure 8 for the corresponding value of J^*. It seems that in the $t-J$ model the n dependence of the transition temperature T_N to antiferromagnetic phase must have an analogous behaviour, because the exact solution of the model (1.2) can serve as a background for an approximate solution of the $t-J$ model.

4 Bethe lattice. The chessboard phase

One can show that in the case of chessboard-like distribution of the localized electrons the equation for the order parameter

$$\delta w = w_A - w_B \tag{4.1}$$

of the chessboard phase can be obtained in analytical form for the model (1.2) on the Bethe lattice. The sublattices A and B are defined by:

$$p_i = e^{i(\mathbf{Q}\mathbf{R}_i)} = \begin{cases} +1, & \mathbf{R}_i \in A \\ -1, & \mathbf{R}_i \in B \end{cases}. \tag{4.2}$$

Indeed, in this inhomogeneous case we have

$$w_i = w + \frac{1}{2}p_i\delta w \qquad n_{i+} \equiv \langle X_i^{++}\rangle = n_+ - \frac{1}{2}p_i\delta n_+, \tag{4.3}$$

where

$$\delta n_+ = n_{B+} - n_{A+}, \tag{4.4}$$

$$w = \frac{1}{2}(w_A + w_B), \qquad n_+ = \frac{1}{2}(n_{A+} + n_{B+}). \tag{4.5}$$

The chemical potential will be defined from the equation

$$n = w + n_+. \tag{4.6}$$

The band Green's function can be represented by

$$\mathcal{G}_s(i,i) = \mathcal{G}_s^{(1)} + p_i\mathcal{G}_s^{(2)}, \tag{4.7}$$

where

$$\mathcal{G}_s^{(1)} = \frac{1}{N}{\sum_{\mathbf{k}}}'\Big\{\mathcal{G}_s(\mathbf{k};\mathbf{k}) + \mathcal{G}_s(\mathbf{k}+\mathbf{Q};\mathbf{k}+\mathbf{Q})\Big\}, \tag{4.8}$$

$$\mathcal{G}_s^{(2)} = \frac{1}{N}{\sum_{\mathbf{k}}}'\Big\{\mathcal{G}_s(\mathbf{k};\mathbf{k}+\mathbf{Q}) + \mathcal{G}_s(\mathbf{k}+\mathbf{Q};\mathbf{k})\Big\} \tag{4.9}$$

$$n_+ = T\sum_s \mathcal{G}_s^{(1)} = \frac{1}{2}\Big(1-w-\frac{1}{2}\delta w\Big)f(\nu)+\frac{1}{2}\Big(1-w+\frac{1}{2}\delta w\Big)f(-\nu)+\frac{4(a^2-b^2)^2}{W^2}\frac{2}{\pi}$$
$$\times\int_0^{\pi/2} dt\frac{\sin^2 t\cos^2 t}{a^2\cos^2 t+b^2\sin^2 t}\Big\{\Big(f[E(t)]+f[-E(t)]\Big)-\Big(f(\nu)+f(-\nu)\Big)\Big\}, \tag{4.23}$$

$$-\frac{1}{2}\delta n_+ = T\sum_s \mathcal{G}_s^{(2)} = \frac{1}{2}\Big(1-w-\frac{1}{2}\delta w\Big)f(\nu)-\frac{1}{2}\Big(1-w+\frac{1}{2}\delta w\Big)f(-\nu)+\frac{4(a^2-b^2)^2}{W^2}\frac{2}{\pi}$$
$$\times\int_0^{\pi/2} dt\frac{\sin^2 t\cos^2 t}{a^2\cos^2 t+b^2\sin^2 t}\Big\{\frac{\nu}{E(t)}\Big(f[E(t)]-f[-E(t)]\Big)-\Big(f(\nu)-f(-\nu)\Big)\Big\}, \tag{4.24}$$

where the summation occurs over the reduced (magnetic) Brillouin zone. The quantities in the right parts of the equations (4.8, 4.9) are the matrix elements of the Fourier transform of $\mathcal{G}_s(i,i')$:

$$\mathcal{G}_s(i,i') = \frac{1}{N}{\sum_{\mathbf{k}}}'\sum_{\alpha,\alpha'}\mathcal{G}_s(\mathbf{k}+\mathbf{Q}_\alpha,\mathbf{k}+\mathbf{Q}_{\alpha'})$$
$$\times e^{i(\mathbf{k}+\mathbf{Q}_\alpha)\mathbf{R}_i - i(\mathbf{k}+\mathbf{Q}_{\alpha'})\mathbf{R}_{i'}} \tag{4.10}$$

where

$$\mathbf{Q}_\alpha = \begin{cases} 0, & \alpha=1 \\ \mathbf{Q}, & \alpha=2 \end{cases}. \tag{4.11}$$

The self-energy part $\Sigma_s(i,i)$ can be written in the form

$$\Sigma_s(i,i) = \Sigma_s^{(1)} + p_i\Sigma_s^{(2)}, \tag{4.12}$$

where in accordance with (2.25)

$$\Sigma_s^{(1)} = -\frac{w\mathcal{G}_s^{(1)}-\frac{1}{2}\delta w\mathcal{G}_s^{(2)}}{\Big[\mathcal{G}_s^{(1)}\Big]^2+\Big[\mathcal{G}_s^{(2)}\Big]^2} \tag{4.13}$$

and

$$\Sigma_s^{(2)} = \frac{w\mathcal{G}_s^{(2)}-\frac{1}{2}\delta w\mathcal{G}_s^{(1)}}{\Big[\mathcal{G}_s^{(1)}\Big]^2+\Big[\mathcal{G}_s^{(2)}\Big]^2}\,. \tag{4.14}$$

Now one can easily obtain the set of equations for $\mathcal{G}_s^{(1)}$ and $\mathcal{G}_s^{(2)}$. After the Fourier transformation (4.10) from the Dyson equation for $\mathcal{G}_s(i,i')$ we have in the case of the Bethe lattice

$$\mathcal{G}_s^{(1)} = \frac{8}{W^2}\frac{\Omega_s}{\overline{\Omega}_s}\Big\{\overline{\Omega}_s-\sqrt{\overline{\Omega}_s^2-W^2/4}\Big\}, \tag{4.15}$$

$$\mathcal{G}_s^{(2)} = \frac{8}{W^2}\frac{\Sigma_s^{(2)}+\frac{1}{2}J^*\delta w}{\overline{\Omega}_s}\Big\{\overline{\Omega}_s-\sqrt{\overline{\Omega}_s^2-W^2/4}\Big\}, \tag{4.16}$$

where

$$\overline{\Omega}_s^2 = \Omega_s^2-\left(\Sigma_s^{(2)}+\frac{1}{2}J^*\delta w\right)^2$$

and

$$\Omega_s = \omega_s - \Sigma_s^{(1)}, \qquad \omega_s \equiv i\omega_s+\mu.$$

After solving the set equations (4.13–4.16) for $\mathcal{G}_s^{(1)}$ and $\mathcal{G}_s^{(2)}$, we have for these quantities:

$$\mathcal{G}_s^{(1)} = \frac{8}{W^2}\omega_s - \frac{\frac{1}{2}\delta w\nu}{\omega_s^2-\nu^2}$$
$$-\frac{\omega_s}{\omega_s^2-\nu^2}\frac{8}{W^2}\sqrt{(\omega_s^2-\omega_1^2)(\omega_s^2-\omega_2^2)}, \tag{4.17}$$

$$\mathcal{G}_s^{(2)} = \frac{8}{W^2}\nu - \frac{\frac{1}{2}\delta w\omega_s}{\omega_s^2-\nu^2}$$
$$-\frac{\nu}{\omega_s^2-\nu^2}\frac{8}{W^2}\sqrt{(\omega_s^2-\omega_1^2)(\omega_s^2-\omega_2^2)}, \tag{4.18}$$

where

$$\nu = \frac{1}{2}\delta w J^*, \tag{4.19}$$

$$\omega_1^2 = \nu^2+b^2, \qquad \omega_2^2 = \nu^2+a^2, \tag{4.20}$$

$$a^2 = \frac{1}{8}W^2\left(1-w+\sqrt{(1-w)^2-(\delta w/2)^2}\right),$$

$$b^2 = \frac{1}{8}W^2\left(1-w-\sqrt{(1-w)^2-(\delta w/2)^2}\right), \tag{4.21}$$

From (4.17, 4.18) we are able to obtain the expression for $Z_s(i,i)G_s^0(i,i)$:

$$Z_s(i,i)G_s^0(i,i) = \frac{1}{2}\left\{1-\frac{W^2}{8}\frac{\frac{1}{2}\delta w}{\omega_s^2-\nu^2}p_i\right.$$
$$\left.+\frac{1}{\omega_s^2-\nu^2}\sqrt{(\omega_s^2-\omega_1^2)(\omega_s^2-\omega_2^2)}\right\}. \tag{4.22}$$

This quantity is necessary for evaluation of λ_i (see Eq. (2.28)).

Using the expressions (4.17, 4.18, 4.22), after some relatively cumbersome calculations we can obtain

See equations (4.23, 4.24) above

$$\lambda_i = -\frac{1}{\pi}\int_0^{\pi/2} dt \frac{a^2\cos^2 t + b^2\sin^2 t + abp_i}{a^2\cos^2 + b^2\sin^2 t} \times \left\{\ln\left(1+e^{\beta[\mu-E(t)]}\right) + \ln\left(1+e^{\beta[\mu+E(t)]}\right) - \ln\left(1+e^{\beta(\mu-\nu)}\right) - \ln\left(1+e^{\beta(\mu+\nu)}\right)\right\}, \quad (4.25)$$

where

$$E(t) = +\sqrt{a^2\cos^2 t + b^2\sin^2 t + \nu^2}. \quad (4.26)$$

Let us represent λ_i in the form

$$\lambda_i = \ln\bigl(1+\exp[\beta(\mu-\nu p_i)]\bigr) - \beta\Theta_i. \quad (4.27)$$

Then the expression (2.27) for w_i is simplified to

$$w_i = \frac{1}{\exp[\beta(\varepsilon_i^f - \mu)]+1}, \quad (4.28)$$

where

$$\varepsilon_i^f = \varepsilon^0 - J^*(n-2w) - \frac{1}{2}J^*\delta n_+ p_i + \Theta_i. \quad (4.29)$$

Now it is easy to compose the equation for the chemical potential μ with the help of (4.6), and to obtain the equation for the order parameter δw. The latter equation has the form

$$\frac{1}{2}\delta w = \left[w(1-w) + \left(\frac{1}{2}\delta w\right)^2\right]\tanh\frac{1}{2}\beta\eta, \quad (4.30)$$

where

$$\eta = J^*\delta n_+ + \Theta_B - \Theta_A. \quad (4.31)$$

Let us consider solutions of the equation (4.30) for some cases. Figure 13 shows the temperature-dependent order parameter δw in the symmetric case for different J^*. At $T = 0$ δw is equal to 1. This is the case of the saturated chessboard phase, when $w_A = 1$ and $w_B = 0$. Let us note that in this case $n_{A+} = 0$, $n_{B+} = 1$ and $\delta n_+ = 1$. At finite temperature the order parameter δw reveals an expected temperature dependence with a continuous phase transition. The general temperature behaviour of δw for different J^* in the symmetric case is similar to that of staggered magnetization for the Heisenberg antiferromagnet in the mean-field approximation.

Away from the symmetric case the temperature behaviour of δw undergoes essential changes that are demonstrated in Figure 14, where the temperature dependence of δw for $J^* = 0.3$, $n = 1$ and different ε^0 is shown. Two regions of varying positive values of ε^0: $0 \le \varepsilon^0 < \varepsilon_c^0$ and $\varepsilon_c^0 < \varepsilon^0 < \varepsilon_*^0$ should be distinguished. (For $n = 1$ the temperature behaviour of δw is invariant when the sign of ε^0 is changed.) The boundary point ε_c^0 for given J^* is

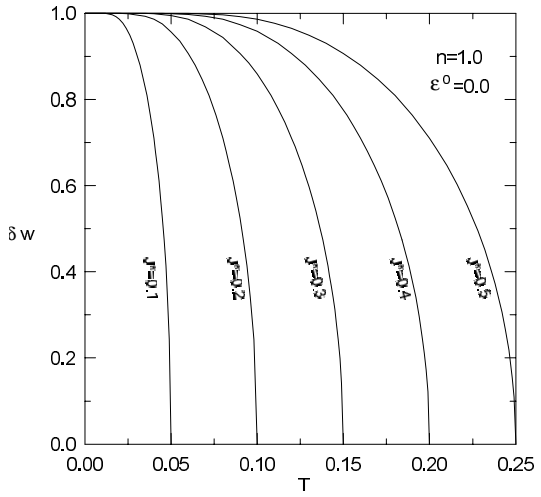

Fig. 13. Temperature dependence of the order parameter δw for different values of J^*.

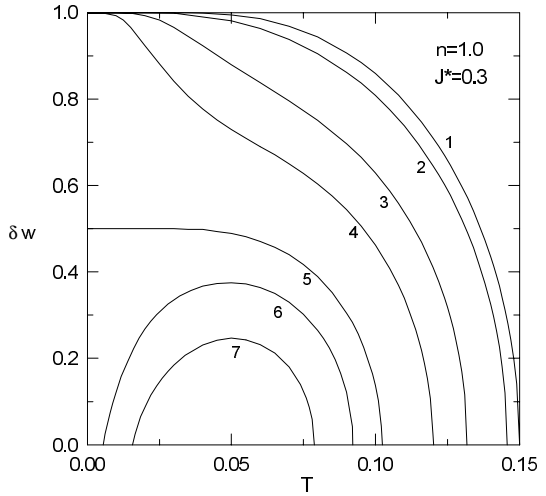

Fig. 14. Temperature dependence of the order parameter δw for different values of ε^0. 1 – $\varepsilon^0 = 0.0$; 2 – $\varepsilon^0 = 0.1$; 3 – $\varepsilon^0 = 0.2$; 4 – $\varepsilon^0 = 0.25$; 5 – $\varepsilon^0 = 0.3$; 6 – $\varepsilon^0 = 0.32$; 7 – $\varepsilon^0 = 0.34$.

determined with the help of Figure 9 or 11 (see the explanation of Fig. 11 in the text). For $J^* = 0.3$, as in the case of Figure 14, the corresponding value of ε^0 is equal to 0.3.

As can be is seen from Figure 14 in the case of $0 \le \varepsilon^0 < \varepsilon_c^0$, the value of δw is equal to 0.5, when $T = 0$. With increase of ε^0 up to $\varepsilon^0 = \varepsilon_c^0$ the temperature dependence of δw attains two flex points (in particular, see the curve 4). At the same time, a strong decrease of $w = 0.5(w_A + w_B)$ at $\varepsilon^0 \to \varepsilon_c^0$ is observed, when temperature is increased. The latter property is clear from a common physical consideration. Let us note that in contrast with the Brandt-Mielsch paper [2], the quantity w is not a fixed parameter in our approach. The fundamental parameters of our theory are the following quantities: T, J^*, n and ε^0. All the other quantities depend on these parameters by force of the corresponding equations.

In the case of $\varepsilon^0 = \varepsilon_c^0 = 0.3$ (see the curve 5) the value of δw is equal to 0.5 when $T = 0$. Here $w_A = 0.5$, $w_B = 0$

and $w = 0.25$. This is the case of the pinning of chemical potential μ at the renormalized level of the A-sublattice's atoms, that is

$$\varepsilon_A^f - \mu = 0. \tag{4.32}$$

The renormalized level of the B-sublattice's atoms is higher in energy then the one of the A-sublattice's atoms, $\Theta_B > \Theta_A$. Therefore, if

$$\varepsilon_B^f - \mu = 0 \tag{4.33}$$

then $w_A = 1$, $w_B = 0.5$ and $w = 0.75$, $\delta w = 0.5$. This case can be realized only for the negative values of ε^0.

Thus, in the chessboard phase at $T = 0$ the quantity w attains only three values: 0.25, 0.5 and 0.75. Accordingly, the order parameter δw can attain two values: 0.5 and 1.0 (see also Refs. [6,7]). The values of w: 0 and 1 are the trivial values. In this case $\delta w = 0$.

Let us return to Figure 14. In the case of $\varepsilon_c^0 < \varepsilon \leq \varepsilon_*^0$ (see also Fig. 11) we have reentrant behaviour of the order parameter, *i.e.* for given ε^0 from the region $\varepsilon_c^0 < \varepsilon^0 \leq \varepsilon_*^0$ we obtain the homogeneous phase at low and high temperatures, and the chessboard phase between some lower critical temperature T_{c1} and some upper critical temperature T_{c2}. The values T_{c1} and T_{c2}, for given J^* and ε^0, can be obtained from Figure 11. In the limit $\varepsilon^0 \to \varepsilon_*^0$ we have $T_{c1} = T_{c2} = T_c^*$ and the chessboard phase disappears

5 Concluding remarks

In the present paper we have considered the strongly correlated Falicov–Kimball model in infinite dimensions. Its Hamiltonian has the form of the simplified $t-J$ model, where electrons with $\downarrow$-spin orientation are localized. With the help of the diagrammatic technique for the Hubbard X-operators we have obtained the set of equations for the band Green's function, and the expression for the $f-f$ susceptibility. These results coincide with the corresponding results of Brandt–Mielsch papers [1,2] in the limit $U \to \infty$. It turns out that in contrast to the Gaussian density of band states utilized by Brandt and Mielsch, one can resolve the above mentioned equations in analytical form for the Bethe lattice with $z \to \infty$, both for the homogeneous phase and for the chessboard-like distribution of localized electrons. In the latter case we have obtained the equation for the order parameter. This equation contains a hyperbolic tangent which is the characteristic quantity for mean-field approximation in models with localized electrons.

It should be noted that the strongly correlated model defined by the Hamiltonian (1.2) can be considered as a test mathematical model for an approximate solution of the $t-J$ model. In recent years the latter model has been used for a investigation of the related high-temperature superconductivity and antiferromagnetism. Meanwhile, one must say that in spite of a great number of papers on this subject the theory of antiferromagnetism in the $t-J$ model is unsatisfactory. Formal mathematical description of antiferromagnetic state is analogous to that of chessboard phase. Therefore, we think that the present paper can be useful for an approximate description of antiferromagnetic state in the $t-J$ model.

It should be also noted that in spite of its simplicity the Falicov–Kimball model reveals a great number of phase states (see Refs. [3,8]). In connection with the abovementioned remark the most interesting among them are the states adjoining to the chessboard phase. These are the state with an incommensurate value of $\mathbf{q}$ (see the formula (2.37)) or the state with different phases coexisting in the mentioned region. It seems that the theory of these states and calculation of the general phase diagram require an additional development. In particular, it is necessary to define more precisely the phase state in the regions near the pure chessboard phase at $T < T_c^*$ for given J^* (see Fig. 11) and in the analogous region in Figure 12. The study of the latter region has a special interest in connection with a possible use of Falicov–Kimball model for an approximate solution of the $t-J$ model.

This work is supported by the State Scientific Program "Modern branches of condensed matter physics", subprogram "Superconductivity", project 95-056.

References

1. U. Brandt, C. Mielsch, Z. Phys. B **75**, 365 (1989).
2. U. Brandt, C. Mielsch, Z. Phys. B **79**, 295 (1989).
3. U. Brandt, C. Mielsch, Z. Phys. B **82**, 37 (1989).
4. P.G. van Dongen, D. Vollhardt, Phys. Rev. Lett. **65**, 1663 (1990).
5. P.G. van Dongen, Phys. Rev. **45**, 2267 (1992).
6. V. Janis, Z. Phys. B **83**, 227 (1991).
7. Q. Si, K. Kotliar, A. Georges, Phys. Rev. B **46**, 1261 (1992).
8. J.K. Freericks, Phys. Rev. B **47**, 9263 (1993).
9. L.M. Falicov, J.Q. Kimball, Phys. Rev. Lett. **22**, 997 (1969).
10. T. Kennedy, E.H. Leeb, Physica A **138**, 320 (1986).
11. U. Brandt, R. Schmidt, Z. Phys. B **63**, 45 (1986).
12. U. Brandt, R. Schmidt, Z. Phys. B **67**, 43 (1987).
13. V. Janis, D. Vollhardt, Int. J. Mod. Phys. B **6**, 731 (1992).
14. D.M. Edwards, J. Phys. Cond. Mat. **5**, 161 (1993).
15. Y.M. Li, N. d'Ambrumenil, Phys. Rev. **49**, 6058 (1994).
16. B.M. Letfulov, Phys. Met. Metallogr., **82**, 590 (1996).
17. Yu. A. Izyumov, B.M. Letfulov, J. Phys. Cond. Mat. **2**, 8905 (1990).
18. Yu. A. Izyumov, B.M. Letfulov, E.V. Shipitsyn, M. Bartkowiak, K.A. Chao, Phys. Rev. B **46**, 15697 (1992).
19. W. Metzner, D. Vollhardt, Phys. Rev. Lett. **62**, 324 (1989).
20. E. Muller-Hartmann, Z. Phys. B **74**, 507 (1989).
21. W. Metzner, P. Schmit, D. Vollhardt, Phys. Rev. B **45**, 2237 (1992).
22. P. Farkaŝovský, Phys. Rev. B **51**, 1507 (1995).
23. P. Farkaŝovský, Phys. Rev. B **4**, 7865 (1996).
24. P.W. Anderson, H. Hasegawa, Phys. Rev. **100**, 675 (1955).
25. B.M. Letfulov, Z. Phys. B (to be published).